

Quantum stochastic transport along chains

Dekel Shapira, Doron Cohen

Department of Physics, Ben-Gurion University of the Negev, Beer-Sheva 84105, Israel

Abstract

The *spreading* of a particle along a chain, and its *relaxation*, are central themes in statistical and quantum mechanics. One wonders what are the consequences of the interplay between *coherent* and *stochastic* transitions. This fundamental puzzle has not been addressed in the literature, though closely related themes were in the focus of the Physics literature throughout the last century, highlighting quantum versions of Brownian motion. Most recently this question has surfaced again in the context of photo-synthesis. Here we consider both an infinite tight-binding chain and a finite ring within the framework of an Ohmic master equation. With added disorder it becomes the quantum version of the Sinai-Derrida-Hatano-Nelson model, which features sliding and delocalization transitions. We highlight non-monotonic dependence of the current on the bias, and a counter-intuitive enhancement of the effective disorder due to coherent hopping.

Introduction

A prototype problem in Physics is the dynamics of a particle along chain that consists of sites. If the dynamics is coherent one expects to observe ballistic motion and Bloch oscillations [1], while for stochastic dynamics one expects to see diffusion and drift. In the presence of disorder, additional fascinating effects emerge: an Anderson localization transition in the coherent problem, and a Sinai-Derrida sliding transition in the stochastic problem. In practical applications the particle can be an exciton [2–4]. Past literature regarding quantum spreading in chains, [5–14], including publications that address the photo-synthesis theme [15–24], were focused mainly on the question how noise and dissipation affect coherent transport. In a sense, our interest is in the reversed question.

In the present work we assume *independent* mechanisms for stochastic asymmetric (dissipative) transitions, and for coherent hamiltonian (conservative) transitions. Such setup is not common: the standard models do not allow to tune on and off the two mechanisms independently. The question arises how the two mechanisms affect each other. Can we simply “sum up” known results for stochastic transport with known results for coherent motion in noisy environment? We shall see that the answer is not trivial. The main surprises come out once we take into account the presence of disorder (see below). An optional way to phrase the question: what is the quantum version of the prototype stochastic problem that is known in the literature as *random walk in*

random environment. As we know from the above cited works, due to disorder, the stochastic dissipative dynamics is not merely a simple minded Brownian motion. We would like to know whether coherence has any implication on the predicted disorder-related crossovers.

We consider a chain whose sites are labeled by x . The particle, or the exciton, can move from site to site (near neighbor transitions only). The transitions are determined by two major parameters: the hopping frequency (c) that controls the coherent hopping; and the fluctuations intensity (ν) that controls the environmentally-induced stochastic transitions. At finite temperature T there is also a dissipation coefficient $\eta = \nu/(2T)$ that is responsible for the asymmetry of the stochastic transitions. On top we might have bias (\mathcal{E}), on-site noisy fluctuations (γ), and different types of disorder. The model is illustrated in Fig.1.

The dynamics is governed by a master equation for the probability matrix

$$\frac{d\rho}{dt} = \mathcal{L}\rho = -i[\mathbf{H}^{(c)}, \rho] + \left(\mathcal{L}^{(B)} + \mathcal{L}^{(S)}\right)\rho \quad (1)$$

where the dissipators $\mathcal{L}^{(B)} \propto \nu$ and $\mathcal{L}^{(S)} \propto \gamma$ are due

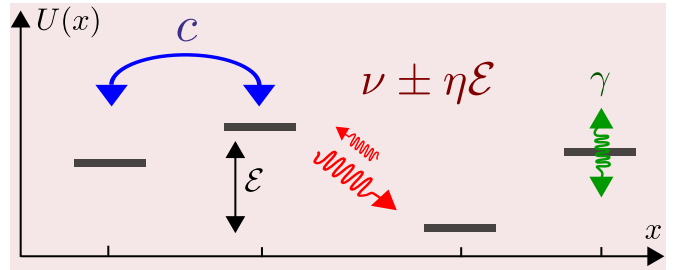


FIG. 1. (1) **Illustration of the model system.** Each site of the chain is represented by a line segment positioned according to its x coordinate and potential $U(x)$. Blue arrow labeled by c represents the possibility for a coherent hopping between two sites. Red arrows represent bath induced stochastic transitions between two sites. The local bath that is responsible for the latter fluctuates with intensity ν , and the induced transitions are asymmetric if $\eta = \nu/(2T)$ is non-zero (finite temperatures). Note that their ratio is $\exp(-\mathcal{E}/T)$ in leading order. The green wiggles represent a local bath that induces fluctuations of intensity γ of the on-site potential. Without the baths it is the Anderson model for coherent transport and localization in disordered chain. In the other extreme, if only the stochastic transitions are present, it is the Sinai-Derrida model for motion in random environment. The latter exhibits a sliding transition as the bias is increased, and an associated Hatano-Nelson delocalization transition once relaxation in a closed ring is considered.

to the interaction with the environment. They are responsible for the stochastic aspect of the dynamics. The Hamiltonian $\mathbf{H}^{(c)}$ contains an on-site potential $U(x)$, and a sum over hopping terms $(c/2)|x \pm 1\rangle\langle x|$. Accordingly it takes the form

$$\mathbf{H}^{(c)} \equiv U(\mathbf{x}) - c \cos(\mathbf{p}) \quad (2)$$

where \mathbf{p} is the momentum operator. The unit of length is the site spacing (x is an integer), and the field is

$$\mathcal{E}_x \equiv -(U(x+1) - U(x)) \quad (3)$$

In the absence of stochastic terms, coherent transport in ordered chain leads to ballistic motion (without bias) and exhibits Bloch-oscillations (with bias). In disordered chain the spreading is suppressed due to Anderson-localization. The effect of noise and dissipation on coherent transport due to $\mathcal{L}^{(S)}$ has been extensively studied. In the Caldeira-Leggett model [25, 26] the interaction is with homogeneous fluctuating environment, leading to Brownian motion with Gaussian spreading. If the interaction is with non-homogeneous fluctuating environment (short spatial correlation scale) the spreading is the sum of a decaying *coherent Gaussian* and a scattered *Stochastic Gaussian* [27]. The tight binding version of this model has been studied in [28]. It has been found that the decoherence and the stochastic-like evolution are dictated by different bands of the Lindblad \mathcal{L} -spectrum that correspond, respectively, to the dephasing and to the relaxation rates in NMR studies of two-level dynamics.

In the other extreme of purely stochastic dynamics, ignoring quantum effects, the disordered model, aka *random walk in random environment*, has been extensively studied by Sinai, Derrida, and followers [29–35]. Without bias the spreading becomes sub-diffusive, while above some critical bias the drift-velocity becomes finite, aka *sliding transition*. Strongly related is the transition from over-damped to under-damped relaxation that has been studied for a finite-size ring geometry [36, 37]. The latter involves *delocalization transition* that has been highlighted for non-hermitian Hamiltonians in the works of Hatano, Nelson and followers [38–45].

One should realize that the two extreme limits of coherent and stochastic spreading have to be bridged within the framework of a model that includes an $\mathcal{L}^{(B)}$ term, not just an $\mathcal{L}^{(S)}$ term. Furthermore, a proper modeling requires the distinction between two types of Master equations. In one extreme we have the *Pauli version*. Traditionally this version is justified by the secular approximation that assumes weak system-bath interaction. In the other extreme we have the *Ohmic version* that assumes short correlation time. The so called “singular coupling limit” can be regarded as an optional way to formalize the short correlation time assumption [46]. Clearly in the mesoscopic context it is more appropriate to adopt the Ohmic version, and regard the Pauli version of the dissipator as a formal approximation.

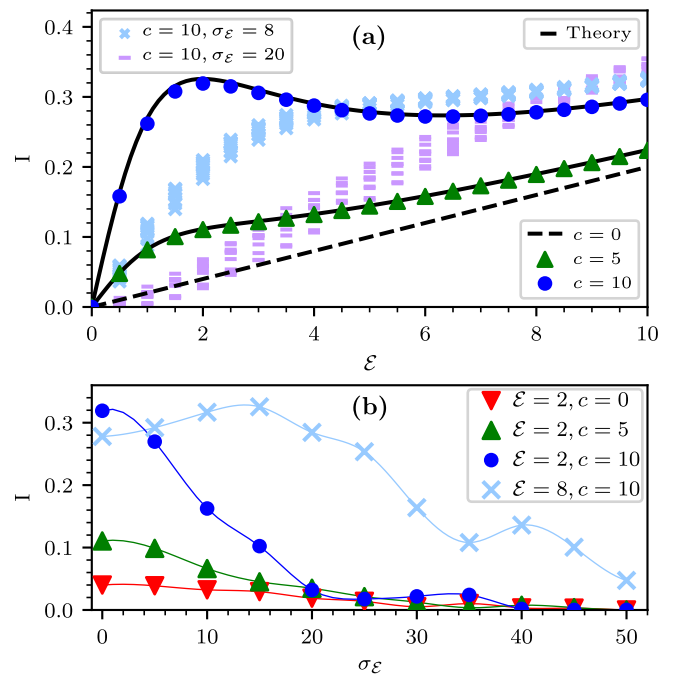


FIG. 2. **The NESS current for a biased chain, with and without disorder.** (a) The NESS current as a function of \mathcal{E} . Black lines are based on equation (17) for clean system with $c=0, 5, 10$ and $\nu=1$ and $\eta=0.01$. Symbols are based on numerical determination of the NESS for a ring of $L=500$ sites. We display 10 independent realizations of the disorder for each value of disorder strength $\sigma_{\mathcal{E}}$, while $c=10$ is kept the same. (b) The average NESS current as a function of $\sigma_{\mathcal{E}}$ for $\mathcal{E}=2$. In the $c=10$ case also for $\mathcal{E}=8$. Thin-lines are a guide to the eye.

Outline.— The model is presented in terms of an Ohmic master equation. The units of time are chosen such that the basic model parameters are $(c, \mathcal{E}, \nu \equiv 1, \eta)$ and the strength of the disorder $\sigma_{\mathcal{E}}$. The interest is in the diffusion coefficient D , the \mathcal{E} -induced drift velocity v , the implied non equilibrium steady state (NESS) current $I \equiv (1/L)v$ for a ring of length L , and the associated Lindblad \mathcal{L} -spectrum. The latter is determined via $\mathcal{L}\rho = -\lambda\rho$, which provides both the relaxation-modes and the decoherence-modes. In particular we observe that the NESS current depends non-monotonically on the bias (Fig. 2a), and that surprisingly it can be enhanced by disorder (Fig. 2b). In a disordered ring, counter-intuitively, relaxation modes become over-damped if coherent transitions are switched on (Fig. 3).

Results

The model.— The isolated chain is defined by the $\mathbf{H}^{(c)}$ Hamiltonian equation (2), that describes a particle or an exciton that can hop along a one-dimensional chain whose sites are labeled by x . The field \mathcal{E}_x might be non-uniform. For the average value of the field we main-

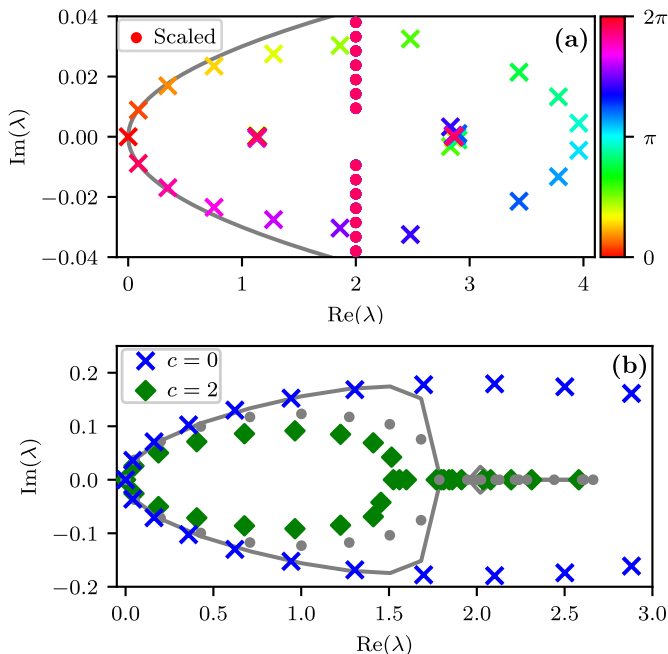


FIG. 3. **The Lindblad \mathcal{L} -spectrum for both non-disordered and disordered rings.** (a) The spectrum for a non-disordered ring of $L = 21$ sites. The eigenvalues that form an ellipse correspond to the stochastic-like relaxation modes. The eigenvalues that bunch together at $\lambda \sim 1, 3$ are the \mp over-damped decoherence modes. The other eigenvalues along $\text{Re}(\lambda) = 2$ correspond to under-damped decoherence modes (each point is in fact a band of L overlapping eigenvalues). The dashed gray-line is based on [equation \(18\)](#). For presentation purpose the eigenvalues marked with dot are scaled by a factor of 0.001 along the vertical axis. The colors indicate the q of each eigenvalue. The parameters are $\nu=1, \eta=0.01, c=0.1, \mathcal{E}=0.5$. (b) The relaxation spectrum with disorder (decoherence modes are excluded). The spectrum for a chain with a given disorder is displayed, once with $c=0$ and once with $c=2$. The gray-circles and the gray-line are the three-band and one-band approximations for $c=2$. The other parameters are $L=31, \mathcal{E}=3, \sigma_{\mathcal{E}}=1.5, \nu=1, \eta=0.03$.

tain the notation \mathcal{E} , while the random component is distributed uniformly (box distribution) within $[-\sigma_{\mathcal{E}}, \sigma_{\mathcal{E}}]$. We regard each pair of neighboring sites as a two-level system [\[S1\]](#). Accordingly we distinguish between two types of terms in the master equation: those that originate from temporal fluctuations of the potential (dephasing due to noisy detuning), and those that are responsible to stochastic transition between the sites (incoherent hopping). The latter are implied by the replacement $(c/2) \mapsto (c/2) + f(t)$ at the pertinent bonds, where $f(t)$ is a bath operator that is characterized by fluctuation intensity ν , and temperature T . Hence the system bath coupling term is $-\mathbf{W}_x f(t)$, where $\mathbf{W}_x = (\mathbf{D}_x + \mathbf{D}_x^\dagger)$ and $\mathbf{D}_x = |x+1\rangle\langle x|$. The baths of different bonds are uncorrelated, accordingly the bond-related dissipator takes the

form

$$\mathcal{L}^{(B)}\rho = -\sum_x \left(\frac{\nu}{2} [\mathbf{W}_x, [\mathbf{W}_x, \rho]] + \frac{\eta}{2} i[\mathbf{W}_x, \{\mathbf{V}_x, \rho\}] \right) \quad (4)$$

where $\eta = \nu/(2T)$ is the friction coefficient, and

$$\mathbf{V}_x \equiv i[\mathbf{H}^{(c)}, \mathbf{W}_x] \quad (5)$$

The friction terms represent the response of the bath to the rate of change of the \mathbf{W}_x . Note that for getting the conventional Fokker-Planck equation the system-bath coupling term would be $-x f(t)$, and \mathbf{V} would become the velocity operator. Here we assume interaction with local baths that in general might have different temperatures. See Methods for some extra technical details regarding the master equation, the nature of the disorder, and the handling of the periodic boundary conditions for the ring configuration.

Pauli-type dynamics.— For pedagogical purpose let us consider first a uniform non-disordered ring without coherent hopping. Furthermore, let us adopt the simplified Pauli-like version of the dissipator (see Methods). Consequently the dynamics of the on-site probabilities $p_x \equiv \rho_{x,x}$ decouples from that of the off-diagonal terms. Namely, one obtains for the probabilities a simple rate equation, where the transition rates between sites are

$$w^\pm = \nu \pm \eta \mathcal{E} \quad (6)$$

in agreement with Fermi-golden-rule (FGR). Note that in leading order $[w^-/w^+] \approx \exp(-\mathcal{E}/T)$ as expected from detailed balance considerations. It follows that the drift velocity and the diffusion coefficient are:

$$v = (w^+ - w^-) = 2\eta \mathcal{E} \quad (7)$$

$$D = \frac{1}{2}(w^+ + w^-) = \nu \quad (8)$$

Consequently one finds two distinct sets of modes: the stochastic-like relaxation modes that are implied by the rate equation for the probabilities, and off-diagonal decoherence modes. The latter share the *same* decay rate $\gamma_0 = w^+ + w^- + \gamma$, where γ stands for optional extra off-diagonal decoherence due to on-site fluctuations. An evolving wavepacket [\[S3\]](#) will decompose into coherent decaying component that is suppressed by factor $e^{-\gamma_0 t}$, and an emerging stochastic component that drifts with velocity v and diffuses with coefficient D .

Full Ohmic treatment.— The state of the particle in the standard representation is given by $\rho_x(r) \equiv \langle x | \rho | x+r \rangle$. The master equation, [equation \(1\)](#) with [equation \(4\)](#), couples the dynamics of the on-site probabilities $p_x \equiv \rho_x(0)$ to that of the off-diagonal elements $\rho_x(r \neq 0)$. The generator \mathcal{L} can be written as a sum of several terms [\[S5\]](#):

$$\mathcal{L} = \mathcal{E} \mathcal{L}^{(\mathcal{E})} + c \mathcal{L}^{(c)} + \nu \mathcal{L}^{(\nu)} + \eta \mathcal{E} \mathcal{L}^{(\mathcal{E})} + \eta c \mathcal{L}^{(c)} \quad (9)$$

Each term is a super-matrix that operates on the super vector $\rho_x(r)$. The first two terms $\mathcal{L}^{(c)}$ and $\mathcal{L}^{(\mathcal{E})}$ arise

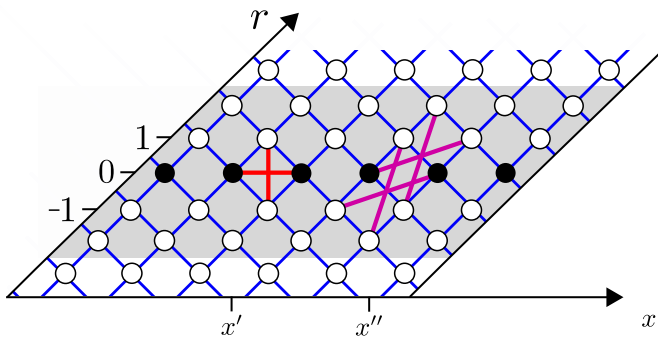


FIG. 4. **Diagrammatic representation of the couplings in the master equation.** A diagonal strip of the probability matrix $\rho_x(r)$ is illustrated. The diagonal elements $p_x = \rho_x(0)$ are represented by filled circles, and the off-diagonal terms by empty circles. The Lindblad generator \mathcal{L} induces “transitions” between the elements. The blue grid lines indicate c -induced couplings. The other couplings within $|r| \leq 2$, indicated by red and purple, are due to a local bath. For presentation purpose (to avoid a crowded set of lines) the red couplings that originate from $\nu\mathcal{L}^{(\nu)}$ and $\eta\mathcal{E}\mathcal{L}^{(\mathcal{E})}$ assume that the local bath is positioned at bond x' , while purple couplings that originate from $\eta c\mathcal{L}^{(c)}$ assume that the bath is positioned at bond x'' .

from the Hamiltonian equation (2). The $\mathcal{L}^{(\nu)}$ term arise from the first term of equation (4), which represent noise-induced transitions. The remaining two friction-terms (proportional to η) arise from equation (5), and correspond to the two terms in the Hamiltonian.

A schematic representation of $\rho_x(r)$ and the couplings is given in Fig.4. The coherent hopping that is generated by $\mathcal{L}^{(c)}$ couples $\rho_x(r)$ to $\rho_x(r\pm 1)$ and to $\rho_{x+1}(r\pm 1)$, while $\mathcal{L}^{(\mathcal{E})}$ contribute “on-site” potential. The noise operator $\nu\mathcal{L}^{(\nu)}$ include the Pauli-terms that were discussed previously, and an additional term that couples the $r = \pm 1$ elements. Together with the friction operator $\eta\mathcal{E}\mathcal{L}^{(\mathcal{E})}$, the Pauli terms induce the asymmetric $x\pm 1$ stochastic transitions of equation (6) along $r=0$. The second friction term $\mathcal{L}^{(c)}$ consists of non-Pauli terms that allow extra $\mathcal{L}^{(c)}$ -type couplings, and in particular extra $x\pm 2$ transitions within the strip $|r| = 0, 1, 2$.

The spectrum for a non-disordered ring.— For a non-disordered ring the super-matrix \mathcal{L} is invariant under x -translations, and therefore we can switch to a Fourier basis where the representation is $\rho(r; q)$. Due to Bloch theorem, the matrix decompose into q -blocks in this basis. Thus in order to find the eigenvalues $\lambda_{q,s}$ and the corresponding eigenmodes we merely have to handle a one dimensional tight binding $|r\rangle$ lattice. See Methods. A representative spectrum is provided in Fig.3a. Consider first the $q=0$ eigenstates. For $q=0$ the c -dependent couplings are zero. For infinite temperature ($\eta=0$) the only non-zero coupling is between $|r = \pm 1\rangle$ due to a non-Pauli term in equation (32). Consequently the $q=0$ block

contains the NESS $|r=0\rangle$ (which is merely the identity matrix in the standard basis), along with a pair of non-trivial decoherence modes $|\pm\rangle$, and a set of uncoupled decoherence modes $|r = \pm 2, \pm 3, \dots\rangle$. The corresponding $\lambda_{q,s}$ eigenvalues (for $\eta=0$) are:

$$\lambda_{0,0} = 0 \text{ (NESS)} \quad (10)$$

$$\lambda_{0,\pm} = 2\nu \pm \sqrt{\nu^2 - \mathcal{E}^2} \quad (11)$$

$$\lambda_{0,s} = 2\nu + i\mathcal{E}s, \quad (s = \pm 2, \pm 3, \dots) \quad (12)$$

The $|\pm\rangle$ modes become over-damped for small bias, while the $|s| > 1$ decoherence modes are always under-damped. Considering the q dependence of the eigenvalues $\lambda_{q,s}$ we get several bands, as illustrated in Fig.3a. Our interest below is in the relaxation modes that are associated with $\lambda_{q,0}$, and determine the long time spreading.

The NESS.— At finite temperature ($\eta > 0$) there are extra couplings that lead to a modified NESS. In leading order the NESS eigenstate is $|0\rangle + \alpha_0|1\rangle + \alpha_0^*|-1\rangle$ with

$$\alpha_0 = \frac{3\nu - i\mathcal{E}}{3\nu^2 + \mathcal{E}^2} \eta c \quad (13)$$

Reverting back to the standard representation we get

$$\rho^{(\text{NESS})} = \frac{1}{L} (\mathbb{1} + \alpha_0 e^{+ip} + \alpha_0^* e^{-ip}) \quad (14)$$

From this we can deduce the steady state momentum distribution [S5], namely, $p(k) \equiv \langle k | \rho^{(\text{NESS})} | k \rangle$. The result in leading order is

$$p(k) \propto \exp \left[\frac{2\eta c}{3\nu^2 + \mathcal{E}^2} (3\nu \cos(k) + \mathcal{E} \sin(k)) \right] \quad (15)$$

For $\mathcal{E} = 0$ this expression is consistent with the canonical expectation $\exp(-\beta \mathbf{H}^{(c)})$.

The current.— For non-zero field ($\mathcal{E} \neq 0$) the NESS momentum distribution is shifted. The expression for the current operator is complicated [S2], but the net NESS current comes out a simple sum of stochastic and coherent terms:

$$I_x = \frac{1}{L} ((w_x^+ - w_x^-) - c \text{Im}(\alpha_0)) \quad (16)$$

$$= \frac{1}{L} \left[1 + \frac{c^2}{6\nu^2 + 2\mathcal{E}^2} \right] 2\eta\mathcal{E} \equiv \frac{1}{L} v \quad (17)$$

We shall further illuminate the physical significance of the second term below. In contrast with the stochastic case, the drift current might be non-monotonic in \mathcal{E} , see Fig.2a. Furthermore, there is a convex range where the second derivative of $I(\mathcal{E})$ is positive.

The *convexity* of the current in some \mathcal{E} range, implies a counter intuitive effect: current may become larger due to disorder. The argument goes as follows: Assume that the sample is divided into two regions, such that \mathcal{E}_x is constant in each region, but slightly smaller (larger) than \mathcal{E} in the first (second) region. Due to the convex property it is implied that the current will be larger. Extending

this argument for a general non-homogeneous (i.e. disordered) field, with the same average bias \mathcal{E} , we expect to observe a *larger* NESS current. This is indeed confirmed in Fig.2a, while additional examples are given and discussed quantitatively in [S6].

The Diffusion.— An optional way to derive equation (17) is to expand $\lambda_{q,0}$ in q , to obtain v . The second order term gives the diffusion coefficient. Namely,

$$\lambda_{q,0} = ivq + Dq^2 + O(q^3) \quad (18)$$

It is therefore enough to determine $\lambda_{q,0}$ via second order perturbation theory with respect to the $q=0$ eigenstates. To leading order in η , a lengthy calculation leads to a result that is consistent with the Einstein relation, namely

$$\frac{v}{D} = \frac{\mathcal{E}}{T}, \quad [\text{valid in leading order}] \quad (19)$$

Thus, to leading order, D is given by equation (8), multiplied by the expression in the square brackets in equation (17). We see that with coherent transitions, for zero bias, this expression takes the form $D = \nu + D_\ell$, where $D_\ell = c^2/(6\nu)$. The latter can be interpreted as a Drude-type result $D_\ell = \ell^2/\tau$, with relaxation time $\tau \sim 1/\nu$ and mean free path $\ell \sim c\tau$. A similar expression has been obtained in [5, 28] for a chain with noisy sites. In the other extreme of large bias equation (8) implies that $D_\ell = (1/2)|c/\mathcal{E}|^2\nu$. This result, like the Drude result, can be regarded as coming from FGR transitions. But now the transitions are between Bloch site-localized states. Namely, we have hopping between neighboring sites ($\ell \sim 1$), with rate of the transitions ($1/\tau$) that is suppressed by a factor $|c/\mathcal{E}|^2$. The suppression factor reflects the first-order-perturbation-theory overlap of Bloch-localized wavefunctions. To summarize: we can say that D_ℓ exhibits a crossover from Drude-type transport to hopping-type transport as the field \mathcal{E} is increased.

In fact we can proceed beyond leading order, and calculate D up to second order in η , see [S5]. Here we cite only the zero bias result:

$$D = \left[1 + \frac{c^2}{6\nu^2} - \frac{c^2}{4T^2} \right] \nu \quad (20)$$

In view of the Drude picture this result is surprising. Namely, one would expect $D_\ell \sim c^2\tau$ to be replaced by $D_\ell \sim \langle v^2 \rangle \tau$, and hence one would expect the replacement $c^2 \mapsto (1 - [1/8](c/T)^2)c^2$ due to the narrowing of the momentum distribution, see Methods. However the current result indicates that the leading correction is related to a different mechanism. Indeed, using a semi-classical perspective, the coupling to the bath involves a $\cos(p)$ factor, see Methods. The zero order diffusion with rate ν arises due to stochastic term in the equation of motion for \dot{x} that involves a $\sin(p)$ factor. Consequently, due to thermal averaging, $\nu \mapsto (1 - [1/8](c/T)^2)\nu$, which explains, up to a factor of 2, the third term in equation (20). We have repeated this calculation also for a

Caldeira-Leggett dissipator, and also for an $\mathcal{L}^{(S)}$ dissipator. For the former the expected (c/T) correction to D_ℓ appears, but has a different numerical factor, while for the latter the correction comes out with an opposite sign. We can show analytically that the discrepancies are due to the modification of the correlation time [47].

Disordered ring.— The so called stochastic field \mathcal{E}_x/T is responsible for the asymmetry of the incoherent transitions. Following Sinai we assume that it has a random component that is (say) box-distributed. From the works of Sinai and Derrida [30–32] we expect a sliding transition as \mathcal{E}/T exceeds a critical value of order $(\sigma_\mathcal{E}/T)^2$. Strongly related is the delocalization transition [36, 38–40, 43, 44] for which the critical value is smaller by a numerical factor. Disregarding this factor we expect

$$\mathcal{E}_c \approx \frac{1}{T}\sigma_\mathcal{E}^2 \quad (21)$$

In the purely stochastic model, for $\mathcal{E} > \mathcal{E}_c$ the relaxation is expected to be under-damped due to a delocalization transition that leads to the appearance of complex eigenvalues at the vicinity of $\lambda = 0$.

The question arises how this transition is affected by quantum coherent hopping. The naive expectation would be to witness a smaller tendency for localization in the relaxation-spectrum because we add coherent bypass that enhances the transport. But surprisingly the numerical results of Fig.3b show that the effect goes in the opposite direction: for non-zero c , some eigenvalues become real, indicating stronger effective disorder.

Enhanced effective disorder.— We turn to provide an explanation for observing enhanced effective disorder due to coherent hopping. On the basis of the non-disordered ring analysis, the relaxation modes occupy mostly the $|r| = 0, 1$ diagonals of ρ , and therefore it makes sense to exclude couplings to the higher diagonals. We verify that this does not change the qualitative picture in Fig.3b (gray vs green symbols). The effect of the $|r| = 1$ band is to introduce virtual coherent transitions between diagonal elements [S7]. Hence we end up with an effective single-band stochastic equation with transition rates

$$w_x^\pm = \nu + \nu_x \pm \eta\mathcal{E}_x \equiv w_x \exp(\pm\tilde{\mathcal{E}}_x) \quad (22)$$

$$\nu_x = \frac{c^2}{2} \frac{\nu - \lambda}{(2\nu - \lambda)^2 + \mathcal{E}_x^2 - \nu^2} \quad (23)$$

The disorder that is associated with ν_x is hermitian, namely, it does not spoil the symmetry of the transitions, it merely implies that we have a tight binding model with random couplings that have some dispersion $\sigma_\perp^2 \equiv \text{Var}(w_x) \propto c^4$. This is known as *resistor network* (RN) disorder. In contrast, the $\pm\eta\mathcal{E}_x$ term induces *asymmetric* transitions. This type of non-hermitian Sinai-type disorder is characterized by the dispersion $\sigma_\parallel^2 \equiv \text{Var}(\tilde{\mathcal{E}}_x)$. The latter translates after non-hermitian gauge transformation to (hermitian) diagonal disorder, with ill-defined

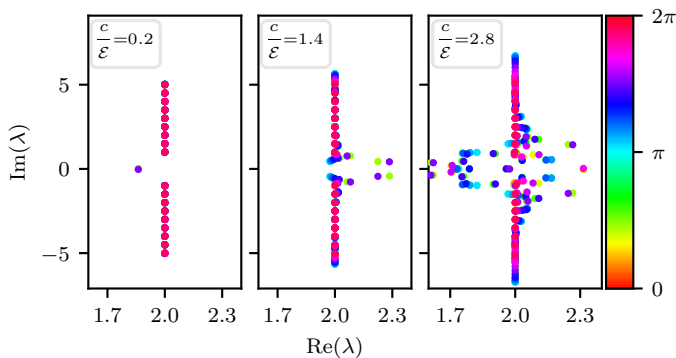


FIG. 5. **Blurring of the Wannier-Stark Ladder.** Here the parameters are $\nu = 1$, $\eta = 0.03$, $\mathcal{E} = 0.5$ and $L = 21$. The parameter c/\mathcal{E} determines the localization range of the Bloch eigenstates. The small q modes are weakly coupled by ν and therefore maintain the \mathcal{E} spacing as implied by equation (12).

boundary conditions. The procedure to handle both types of disorder has been discussed in [36] following [39]. One defines an hermitian RN matrix by setting $\tilde{\mathcal{E}}_x=0$ in equation (22). The RN matrix has a real spectrum with eigenstates that are characterized by inverse localization length that is dominated by the RN-disorder, namely, $\kappa(\lambda) \propto \sigma_{\perp}^2 \lambda$. Adding back the field \mathcal{E}_x , the eigenstates remain localized (with real eigenvalues) only in regions where localization is strong enough, that is, $\kappa(\lambda) > \mathcal{E}/T$. Estimating σ_{\perp} , see [S7] for an explicit expression, we deduce that the additional RN disorder is responsible for the observed numerical result.

The Wannier-Stark Ladder.— We shift our attention to the full Lindblad spectrum. In the absence of coupling to the bath, the eigenstates of the Hamiltonian equation (2) are Bloch localized. Each eigenstate occupies a spatial region $\sim c/\mathcal{E}$, and the corresponding eigenenergies form a ladder with spacing \mathcal{E} , that reflects the frequency of the Bloch oscillations. Weak coupling to the bath leads to damping of the Bloch oscillations. This is reflected by the Lindblad spectrum. For the $q = 0$ modes we have obtained equation (12), where we see that the eigenvalues acquire a real part, but maintain the ladder structure. But for non-zero q the $\mathcal{L}^{(c)}$ term couples the modes to the perturbation that is created at the $|r| < 2$ region by $\mathcal{L}^{(\nu)}$, see equation (31) and equation (32) of the Methods. This results in a deformation of the ladder. Namely, the ladder consists of bands, and the number of bands that are deformed equals the Bloch localization length. See Fig.5.

Regime diagram.— We would like to place our results in the context of the vast quantum dissipation literature. The prototype model of Quantum Brownian Motion (QBM), aka the Caldeira-Leggett model, involves coupling to a single bath that exerts a fluctuating homogeneous field of force. In the classical framework it leads

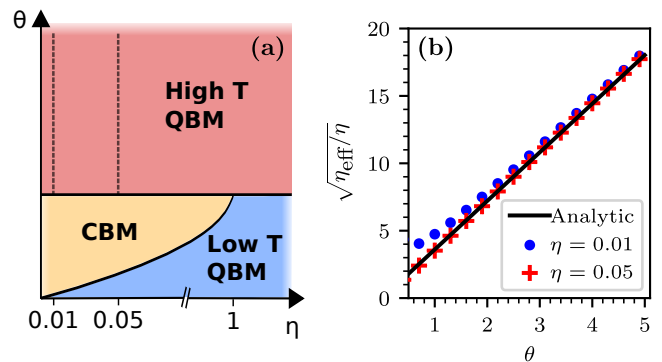


FIG. 6. **The Brownian Motion regime diagram.** (a) The various regions in the (η, θ) diagram are indicated. We distinguish between the Classical-like Brownian Motion (CBM) region; the low-temperature QBM region where memory effects dominates; and the high-temperature QBM region that has been discussed in this article. The Lindblad correction to the Ohmic master equation is negligible above the solid $\theta \sim 1$ line. (b) The effective friction coefficient η_{eff} of equation (27) is determined numerically along the two dashed lines of panel (a), and compared with the analytical prediction of equation (17). The parameters are $\nu = 1$, $\mathcal{E} = 0.5$ and $L = 500$. For lower θ , the Lindblad correction becomes important (not shown).

to the standard Langevin equation

$$m\ddot{x} = \mathcal{E} - \eta\dot{x} + f(t) \quad (24)$$

and equation (1) becomes the standard Fokker Planck equation. In the tight-binding framework we have the identification $m \mapsto 1/(ca^2)$, where a is the lattice constant. The standard QBM model features a single dimensionless parameter, the scaled inverse temperature β , which is the ratio between the thermal time $1/T$ and damping time m/η . In the lattice problem we can define two dimensionless parameters

$$\alpha = \frac{1}{2\pi}\eta a^2 \quad \text{scaled friction} \quad (25)$$

$$\theta = \frac{T}{c} = \frac{\nu}{2\eta c} \quad \text{scaled temperature} \quad (26)$$

Accordingly $\beta = \alpha/\theta$. Note that in our model we set the units such that $a = 1$, hence, disregarding 2π factor, our scaled friction parameter η is the same as α .

The standard analysis of QBM [48] reveals that quantum-implied memory effects are expressed in the regime $\beta \gg 1$, where a transient $\log(t)$ spreading is observed in the absence of bias, followed by diffusion. Most of the quantum dissipation literature, regarding the two-site spin-boson model [49] and regarding multi-site chains [50, 51], is focused in this low temperature regime, where significant deviations from the classical predictions are observed for large α of order unity. In contrast, our interest is in the $\alpha, \beta \ll 1$ regime.

Our (η, θ) regime diagram Fig.6 is roughly divided into two regions by the line $\theta \sim 1$. Along this line the thermal de-Broglie wavelength of the particle is of order of the lattice constant, hence it bears formal analogy to the analysis of QBM in cosine potential [52], where it marks the border to the regime where activation mechanism comes into action. In our tight binding model we have a single band, hence transport via thermal activation is not possible. Rather, in the $\theta > 1$ regime, where $T \gg c$, the momentum distribution within the band is roughly flat, and the drift is dictated by equation (17), that is,

$$v = 2\eta\mathcal{E} + \frac{1}{\eta_{\text{eff}}}\mathcal{E} \quad (27)$$

where $\eta_{\text{eff}} \approx 12\theta^2\eta$ for weak field. The low temperature regime $\theta \ll 1$ has not been addressed in this work, because the Ohmic master equation fails to reproduce canonical equilibration in this regime (see Methods). Still we would like to illuminate what we get (not presented) if this aspect is corrected. In the regime $\theta \ll 1$ the momentum distribution becomes much narrower (only low energy momenta are populated) and therefore $\eta_{\text{eff}} \sim \eta$ as implied by equation (24). This we call Classical-like Brownian motion (CBM) regime. Once the coupling to the bath is not the simple x -coupling of the Caldeira-Leggett model, a numerical prefactor is expected (see Methods for detailed argument).

Discussion

There is a rich literature regarding Quantum Brownian motion (see [48, 53–55] and references within). In the condensed matter literature it is common to refer to the Caldeira-Leggett model [25, 26], where the particle is linearly coupled to a bath of harmonic oscillators that mimic an Ohmic environment. Some works study the motion of a particle in a periodic potential, possibly with bias, aka washboard potential [51, 52, 56], while other refer to tight binding models [6, 50, 57] as in this work. The focus in those papers is mostly on non-Markovian effects: at low temperatures the fluctuations are not like “white noise”, and are dominated by a high frequency cutoff ω_c . Consequently the handling of long-time correlations becomes tricky. In this context the low temperature dependence of the diffusion and the mobility is modified for $\alpha > 1/2$ and $\alpha > 1$.

The line of study in the above models has assumed that the fluctuations that are induced by the bath are uniform in space. In some other works the dynamics of a particle that interacts with local baths has been considered. In such models the fluctuations acquire finite correlation length in space [5, 7–14, 27, 28]. The extreme case, as in this work, are tight binding models where the coupling is to uncorrelated baths that seat on different sites or bonds. Studies in this context assume bath that are connected at the end points [58], or baths that act as noise

source [5]. Ref. [28] has analyzed the spectral properties for a chain with noisy sites, Ref. [9] has considered colored noise sources strongly coupled to each site, Ref. [59] has considered noisy transitions on top of coherent transitions, Ref. [60] has considered transport in the presence of dephasing and disorder, Ref. [11] has considered numerically transport properties of a noisy system with static disorder, and [61] has addressed some bounds in the absence of disorder. The basic question of transport in a tight-binding models has resurfaced in the context of excitation transport in photosynthetic light-harvesting complexes [15–24].

It is quite surprising that all of the above cited works have somehow avoided the confrontation with themes that are familiar from the study of stochastic motion in random environment. Specifically we refer here to the extensive work by Sinai, Derrida, and followers [29–35], and the studies of stochastic relaxation [36, 37] which is related to the works of Hatano, Nelson and followers [36–45]. Clearly we have here a gap that should be bridged.

In this article we have studied transport properties along a chain taking into account several themes that have not been combined in past studies: **(a)** The baths on different bonds are not correlated in space; **(b)** The baths are not just noise - the temperature is high but finite; **(c)** Without coherent hopping it is the Sinai-Derrida-Hatano-Nelson model which exhibits sliding and delocalization transitions; **(d)** Without baths it is a disordered chain with Anderson localization; **(e)** The bias might be large such that Bloch dynamics is reflected.

The “small” parameter in our analysis is the inverse temperature. The following observations have been highlighted: **(1)** The NESS current is the sum of stochastic and quasi-coherent terms; **(2)** It displays non-monotonic dependence on the bias, as shown in Fig. 2, due to crossover from Drude-type to hopping-type transport; **(3)** Disorder may increase the current due to convex property; **(4)** The interplay of stochastic and coherent transition is reflected in the Lindblad spectrum; **(5)** In the presence of disorder the quasi-coherent transitions enhance the localization of the relaxation modes. Thus, with regard to the Sinai-Derrida sliding transition, and the strongly related Hatano-Nelson delocalization transition, we find that adding coherent transitions “in parallel” have in some sense opposite effects: on the one hand they add bypass for the current (point (1) above), but on the other hand they enhance the tendency towards localization (point (5) above). Some of our results might be relevant to studies of optimal transport efficiency [R1, R2] and the quantum Goldilocks effect [R3].

Methods

Master equation for disordered chain.— A pedagogical presentation of the procedure for the construction of an Ohmic master equation for a two site system, and

then for a chain, is presented in [S1]. Each bond has a different bath, and therefore can experience different temperature and friction. Accordingly we can have disorder that originates either from the Hamiltonian (say random \mathcal{E}_x as assumed in the main text), or from having different baths (random ν_x or random η_x). This extra disorder can be incorporated in a straightforward manner, and does not affect the big picture.

Thermalization.— The Ohmic master equation for a Brownian particle, if the coupling to the bath were $-\mathbf{x}f(t)$, is the standard Fokker-Plank equation. It leads to canonical thermal state for any friction and for any temperature. This is not the case for a discrete two level system. The agreement with the canonical result is guaranteed only to first order in η . This is reflected in equation (6). The same applies for a chain. Note that in this sense the Ohmic approximation is very different from the secular or Pauli approximation [62], or specially constructed Davies Liouvillian [63], that guarantee canonical thermalization.

It is important to identify the “small parameter” that controls the deviation from canonical thermalization. The standard coupling via \mathbf{x} induce transitions between neighboring momenta, and therefore the small parameter is Δ/T , where the level spacing Δ goes to zero in the $L \rightarrow \infty$ limit. But for local baths, the coupling is to $\delta(\mathbf{x} - x_\alpha)$ scatterers, that create transitions to all the levels within the band. Therefore the small parameter in the absence of bias is c/T . This assertion is confirmed numerically by inspection of the equilibrium momentum distribution $p(k)$, see [S5]. We conclude that in the regime of interest ($\theta > 1$) the Ohmic master equation can be trusted, while for lower temperatures we have to “correct” it. For the two site system the “corrected” equation is the Bloch equation, where the ratio of the rates is in agreement with detailed balance (not just in leading order in η). For a chain, we cannot justify the secular approximation, and therefore the correction procedure is ill defined.

The friction coefficient.— In the Caldeira-Leggett model for Brownian particle, with interaction term $-\mathbf{x}f(t)$, the bath induced fluctuations $f(t)$ are determined by a coupling constant η , and by the bath temperature T , such that at high temperatures the intensity of the fluctuations is $\nu = 2\eta T$. The η parameter is defined such that the friction coefficient in equation (24) equals η . A straightforward generalizations [27] shows that for interaction with local baths $\sum_\alpha u_\alpha(\mathbf{x})f_\alpha(t)$, with $u_\alpha(x) = u(x - x_\alpha)$, the effective friction coefficient is $\eta_{\text{eff}}(x) = \eta \sum_\alpha [u'_\alpha(x)]^2$. For homogeneous distribution of local baths that have the same η , the friction coefficient becomes x -independent. In the model under consideration the coupling to the baths is $\sum_\alpha \mathbf{W}_\alpha f_\alpha(t)$, where α labels the sites. Disregarding commutation, it can be

written as $2 \cos(\mathbf{p}) \sum_\alpha u_\alpha(\mathbf{x})f_\alpha(t)$, where the u -s are site localized. It follow that the effective friction coefficient is momentum dependent, namely $\eta_{\text{eff}} \sim |\cos(p)|^2 \eta$. But for equilibration in the $\theta < 1$ regime only low momenta are important hence we expect, up to numerical prefactor to observe $\eta_{\text{eff}} \approx \eta$. The failure to observe this result is due to improper thermalization, as discussed in a previous paragraph.

Positivity.— Irrespective of η , there is another complication with the Ohmic master equation. If the temperature is low (small ν) the relaxation may lead to a sub-minimal wavepacket that violates the uncertainty principle. This reflects the observation that the Ohmic master equation is not of Lindblad form, and violates the *positivity* requirement. The minimal correction required to restore positivity is to couple \mathbf{V} to an extra noise source of intensity

$$\nu_\eta = \frac{\nu}{(4T)^2} = \frac{\eta^2}{4\nu} \quad (28)$$

This term is essential in the low temperature regime. We have verified numerically that the extra noise term can be neglected in the high temperature regime where our interest is focused.

On-site dissipators.— The model of [28] combines Hamiltonian term with dissipator of the $\mathcal{L}^{(S)}$ type that originates from couplings via $\mathbf{W}_x := \mathbf{Q}_x$, where $\mathbf{Q}_x = |x\rangle\langle x|$. Such dissipator leads to off-diagonal dephasing that is generated by $\mathbf{Q}_x \rho \mathbf{Q}_x$ terms, and therefore excludes the possibility for inter-site stochastic transitions. Similar remark applies to the familiar Caldeira-Leggett model of Quantum Brownian motion [25], where the coupling is via $\mathbf{W} := \mathbf{x}$. Namely, it is a single bath that exerts a fluctuating homogeneous force that affects equally all the sites, as in [50]. In our model the dissipation effect is local: many uncorrelated local baths.

Pauli dissipator.— A conventional Pauli-type dissipator is obtained if we drop some of the terms in the Ohmic dissipator of equation (4). Namely,

$$\begin{aligned} \mathcal{L}^{(\text{Pauli})} \rho &= -(w^+ + w^-) \rho \\ &+ \sum_x (w^+ \mathbf{D}_x^\dagger \rho \mathbf{D}_x + w^- \mathbf{D}_x \rho \mathbf{D}_x^\dagger) \\ &- \gamma \left(\rho - \sum_x \mathbf{Q}_x \rho \mathbf{Q}_x \right) \end{aligned} \quad (29)$$

The transition rates between sites, $w^\pm = [\nu \pm \eta \mathcal{E}]$, are in agreement with FGR. For completeness, we added here a γ term that represents optional off-diagonal decoherence due to on-site noise.

Ring configuration.— For numerical treatment, and for the purpose of studying relaxation dynamics, we close the chain into a ring. This means to impose periodic boundary conditions. With uniform field \mathcal{E} , one encounter a huge potential drop at the boundary. To avoid this complication we assume that the boundary bond has an infinite temperature, hence the formation of a stochastic barrier is avoided, and the circulation of the stochastic field (aka *affinity*) becomes \mathcal{E}/T as desired. In the analytical treatment of a clean ring we assume that ν , and η and \mathcal{E} in the master equation are all uniform, such that invariance under translation is regained. This cheat is valid for large ring if ρ is banded, reflecting a finite spatial correlation scale. See numerical verification in [S2].

The Bloch eigenstates of a clean ring.— The \mathcal{L} super-operator in the Bloch $(r; q)$ basis, decomposes into q Blocks. Each block can be written as a sum of terms, as in equation (9), that operate over a one dimensional tight binding $|r\rangle$ lattice. In this representation the coherent dynamics is generated by

$$\mathcal{L}^{(\mathcal{E})} = -i \sum_r |r\rangle r \langle r| \quad (30)$$

$$\mathcal{L}^{(c)} = \sin(q/2)[\mathcal{D}_\perp^\dagger - \mathcal{D}_\perp] \quad (31)$$

where $\mathcal{D}_\perp = \sum_r |r+1\rangle \langle r|$. For the ν induced stochastic transitions we have

$$\mathcal{L}^{(\nu)} = -2 + 2 \cos(q)|0\rangle\langle 0| \quad (32)$$

$$+ (|1\rangle\langle -1| + |-1\rangle\langle 1|) \quad (33)$$

where the last term is non-Pauli. The Pauli-type friction term takes the form:

$$\mathcal{L}^{(\tilde{\mathcal{E}})} = -2i \sin(q)|0\rangle\langle 0| \quad (34)$$

And the additional friction terms are:

$$\mathcal{L}^{(\tilde{c})} = \frac{1}{2} \cos(q/2)[\mathcal{D}_\perp + \mathcal{D}_\perp^\dagger] \quad (35)$$

$$+ \frac{1}{2} \cos(3q/2) [| \pm 1\rangle\langle 0| - |0\rangle\langle \pm 1|] \quad (36)$$

$$+ \frac{1}{2} \cos(q/2) [| \mp 2\rangle\langle \pm 1| - | \pm 1\rangle\langle \mp 2|] \quad (37)$$

Note that the zero eigenvalue belongs to the $q = 0$ block. Some more details are provided in [S5].

Diffusion at finite temperature.— The Drude type term in the expression for the diffusion equation (20) is up to numerical prefactor $\langle v_k^2 \rangle \tau$, where $\langle v_k^2 \rangle = c^2/2$ for uniform momentum distribution. At finite temperature this distribution equation (15) is not uniform. Here we consider zero bias and get

$$\langle v_k^2 \rangle = \int_{-\pi}^{\pi} [c \sin(k)]^2 p(k) dk \approx \left[1 - \frac{1}{8}(\beta c)^2 \right] \frac{c^2}{2} \quad (38)$$

where $\beta = 1/T$, and recall that $\eta = \nu/(2T)$. The analytical calculation in [S5] leads to a different result which implies that the expression in the square brackets should be replaced by $[1 - 6\eta^2]$, which means that the relevant dimensionless parameter is ν/T and not c/T . Fig.S4 of [S5]b confirms this statement.

Acknowledgment.— This research was supported by the Israel Science Foundation (Grant No.283/18).

-
- [R1] Optimal transport in one-dimensional infinite chains has been studied in [5–7, 9, 18, 19].
- [R2] Optimal transport in one-dimensional chains with “exit site” has been studied in [12–14].
- [R3] The term quantum Goldilocks effect has been suggested in [10], for the idea that natural selection tends to drive quantum systems to the degree of optimal quantum coherence for transport.
- [S1] See SM sections 1 and 2 for pedagogical presentation of the procedure for the construction of an Ohmic master equation for 2 a site system and for a chain.
- [S2] See SM section 3 for an explicit expression for the current operator.
- [S3] See SM section 4 for pedagogical summary regarding spreading, following [27].
- [S4] See SM section 4 for technical summary of the procedure for finding the eigenvalues of a master equation with a Pauli-type dissipator. It follows [28], but here we include additional stochastic transitions in “parallel” to the coherent hopping, and incorporate also the bias within a first order treatment.
- [S5] See SM sections 5-7 for technical details regarding the procedure for finding the eigenmodes of the Ohmic master equation, including explicit expressions for the η related terms in the Fourier representation, numerical verification for momentum thermalization, and derivation of the associated η -related correction for the diffusion coefficient.
- [S6] See SM section 3 for extra numerics that concerns the calculation of the current for a disordered chain, and the manifestation of the convex property.
- [S7] See SM section 8 for technical details regarding the derivation of the effective disorder that emerges in the reduced rate equation due to virtual coherent transitions.
- [1] T Hartmann, F Keck, H J Korsch, and S Mossmann, “Dynamics of Bloch oscillations,” *New Journal of Physics* **6**, 2–2 (2004).
- [2] Francois Dubin, Romain Melet, Thierry Barisien, Roger Grousson, Laurent Legrand, Michel Schott, and Valia Voliotis, “Macroscopic coherence of a single exciton state in an organic quantum wire,” *Nature Physics* **2**, 32 (2006).
- [3] Tammie R Nelson, Dianelys Ondarse-Alvarez, Nicolas Oldani, Beatriz Rodriguez-Hernandez, Laura Alfonso-Hernandez, Johan F Galindo, Valeria D Kleiman, Sebastian Fernandez-Alberti, Adrian E Roitberg, and Sergei Tretiak, “Coherent exciton-vibrational dynamics and energy transfer in conjugated organics,” *Nature communications* **9**, 2316 (2018).
- [4] Thomas Dekorsy, Albrecht Bartels, Heinrich Kurz, Klaus Köhler, Rudolf Hey, and Klaus Ploog, “Coupled Bloch-phonon oscillations in semiconductor superlattices,” *Physical review letters* **85**, 1080 (2000).
- [5] A Madhukar and W Post, “Exact solution for the diffusion of a particle in a medium with site diagonal and off-diagonal dynamic disorder,” *Physical Review Letters* **39**, 1424 (1977).
- [6] Ulrich Weiss and Hermann Grabert, “Quantum diffusion of a particle in a periodic potential with ohmic dissipation,” *Physics Letters A* **108**, 63–67 (1985).
- [7] N. Kumar and A. M. Jayannavar, “Quantum diffusion in thin disordered wires,” *Phys. Rev. B* **32**, 3345–3347 (1985).
- [8] Dibyendu Roy, “Crossover from ballistic to diffusive thermal transport in quantum Langevin dynamics study of a harmonic chain connected to self-consistent reservoirs,” *Physical review. E, Statistical, nonlinear, and soft matter physics* **77**, 062102 (2008).
- [9] Ariel Amir, Yoav Lahini, and Hagai B Perets, “Classical diffusion of a quantum particle in a noisy environment,” *Physical Review E* **79**, 050105 (2009).
- [10] Seth Lloyd, Masoud Mohseni, Alireza Shabani, and Herschel Rabitz, “The quantum Goldilocks effect: on the convergence of timescales in quantum transport,” *arXiv:1111.4982* (2011).
- [11] Jeremy M Moix, Michael Khasin, and Jianshu Cao, “Coherent quantum transport in disordered systems: I. the influence of dephasing on the transport properties and absorption spectra on one-dimensional systems,” *New Journal of Physics* **15**, 085010 (2013).
- [12] Jianlan Wu, Robert J. Silbey, and Jianshu Cao, “Generic mechanism of optimal energy transfer efficiency: A scaling theory of the mean first-passage time in exciton systems,” *Phys. Rev. Lett.* **110**, 200402 (2013).
- [13] Yang Zhang, G. Luca Celardo, Fausto Borgonovi, and Lev Kaplan, “Opening-assisted coherent transport in the semiclassical regime,” *Phys. Rev. E* **95**, 022122 (2017).
- [14] Yang Zhang, G. Luca Celardo, Fausto Borgonovi, and Lev Kaplan, “Optimal dephasing for ballistic energy transfer in disordered linear chains,” *Phys. Rev. E* **96**, 052103 (2017).
- [15] Herbert van Amerongen, Rienk van Grondelle, and Leonas Valkunas, *Photosynthetic Excitons* (WORLD SCIENTIFIC, 2000).
- [16] Thorsten Ritz, Ana Damjanović, and Klaus Schulten, “The quantum physics of photosynthesis,” *ChemPhysChem* **3**, 243–248 (2002).
- [17] Yuan-Chung Cheng and Graham R. Fleming, “Dynamics of light harvesting in photosynthesis,” *Annual Review of Physical Chemistry* **60**, 241–262 (2009).
- [18] Martin B Plenio and Susana F Huelga, “Dephasing-assisted transport: quantum networks and biomolecules,” *New Journal of Physics* **10**, 113019 (2008).
- [19] Patrick Rebentrost, Masoud Mohseni, Ivan Kassal, Seth Lloyd, and Alán Aspuru-Guzik, “Environment-assisted quantum

- transport,” *New Journal of Physics* **11**, 033003 (2009).
- [20] Patrick Rebentrost, Masoud Mohseni, and Aln Aspuru-Guzik, “Role of quantum coherence and environmental fluctuations in chromophoric energy transport,” *The Journal of Physical Chemistry B* **113**, 9942–9947 (2009).
- [21] Mohan Sarovar and K Birgitta Whaley, “Design principles and fundamental trade-offs in biomimetic light harvesting,” *New Journal of Physics* **15**, 013030 (2013).
- [22] KDB Higgins, SC Benjamin, TM Stace, GJ Milburn, Brendon William Lovett, and EM Gauger, “Superabsorption of light via quantum engineering,” *Nature communications* **5**, 4705 (2014).
- [23] Giuseppe L Celardo, Fausto Borgonovi, Marco Merkli, Vladimir I Tsifrinovich, and Gennady P Berman, “Superradiance transition in photosynthetic light-harvesting complexes,” *The Journal of Physical Chemistry C* **116**, 22105–22111 (2012).
- [24] Heechul Park, Nimrod Heldman, Patrick Rebentrost, Luigi Abbondanza, Alessandro Iagatti, Andrea Alessi, Barbara Patrizi, Mario Salvalaggio, Laura Bussotti, Masoud Mohseni, *et al.*, “Enhanced energy transport in genetically engineered excitonic networks,” *Nature materials* **15**, 211 (2016).
- [25] Amir O Caldeira and Anthony J Leggett, “Path integral approach to quantum brownian motion,” *Physica A: Statistical mechanics and its Applications* **121**, 587–616 (1983).
- [26] Amir O Caldeira and Anthony J Leggett, “Quantum tunnelling in a dissipative system,” *Annals of Physics* **149**, 374 – 456 (1983).
- [27] Doron Cohen, “Unified model for the study of diffusion localization and dissipation,” *Physical Review E* **55**, 1422 (1997).
- [28] Massimiliano Esposito and Pierre Gaspard, “Emergence of diffusion in finite quantum systems,” *Journal of statistical physics* **121**, 463–496 (2005).
- [29] Freeman J. Dyson, “The dynamics of a disordered linear chain,” *Phys. Rev.* **92**, 1331–1338 (1953).
- [30] Ya. G. Sinai, “The limiting behavior of a one-dimensional random walk in a random medium,” *Theory of Probability & Its Applications* **27**, 256–268 (1983).
- [31] B Derrida and Ya Pomeau, “Classical diffusion on a random chain,” *Physical Review Letters* **48**, 627 (1982).
- [32] Bernard Derrida, “Velocity and diffusion constant of a periodic one-dimensional hopping model,” *Journal of Statistical Physics* **31**, 433–450 (1983).
- [33] Shlomo Havlin and Daniel Ben-Avraham, “Diffusion in disordered media,” *Advances in Physics* **36**, 695–798 (1987).
- [34] J-Ph Bouchaud, A Comtet, A Georges, and P Le Doussal, “Classical diffusion of a particle in a one-dimensional random force field,” *Annals of Physics* **201**, 285–341 (1990).
- [35] Jean-Philippe Bouchaud and Antoine Georges, “Anomalous diffusion in disordered media: Statistical mechanisms, models and physical applications,” *Physics Reports* **195**, 127 – 293 (1990).
- [36] Daniel Hurowitz and Doron Cohen, “Percolation, sliding, localization and relaxation in topologically closed circuits,” *Scientific reports* **6** (2016).
- [37] Daniel Hurowitz and Doron Cohen, “Relaxation rate of a stochastic spreading process in a closed ring,” *Phys. Rev. E* **93**, 062143 (2016).
- [38] Naomichi Hatano and David R. Nelson, “Localization transitions in non-hermitian quantum mechanics,” *Phys. Rev. Lett.* **77**, 570–573 (1996).
- [39] Naomichi Hatano and David R. Nelson, “Vortex pinning and non-hermitian quantum mechanics,” *Phys. Rev. B* **56**, 8651–8673 (1997).
- [40] Naomichi Hatano, “Localization in non-hermitian quantum mechanics and flux-line pinning in superconductors,” *Physica A: Statistical Mechanics and its Applications* **254**, 317–331 (1998).
- [41] David K. Lubensky and David R. Nelson, “Pulling pinned polymers and unzipping dna,” *Physical review letters* **85**, 1572–5 (2000).
- [42] David K. Lubensky and David R. Nelson, “Single molecule statistics and the polynucleotide unzipping transition,” *Phys. Rev. E* **65**, 031917 (2002).
- [43] Ariel Amir, Naomichi Hatano, and David R Nelson, “Localization in non-hermitian chains with excitatory/inhibitory connections,” arXiv preprint arXiv:1512.05478 (2015).
- [44] Ariel Amir, Naomichi Hatano, and David R Nelson, “Non-hermitian localization in biological networks,” *Physical Review E* **93**, 042310 (2016).
- [45] Karin A. Dahmen, David R. Nelson, and Nadav M. Shnerb, “Population dynamics and non-Hermitian localization,” in *Statistical Mechanics of Biocomplexity*, edited by D. Reguera, J.M.G. Vilar, and J.M. Rubí (Springer Berlin Heidelberg, Berlin, Heidelberg, 1999) pp. 124–151.
- [46] Ángel Rivas and Susana F Huelga, *Open Quantum Systems* (Springer, 2012).
- [47] Dekel Shapira and Doron Cohen, In preparation.
- [48] Vincent Hakim and Vinay Ambegaokar, “Quantum theory of a free particle interacting with a linearly dissipative environment,” *Phys. Rev. A* **32**, 423–434 (1985).
- [49] A. J. Leggett, S. Chakravarty, A. T. Dorsey, Matthew P. A. Fisher, Anupam Garg, and W. Zwerger, “Dynamics of the dissipative two-state system,” *Rev. Mod. Phys.* **59**, 1–85 (1987).
- [50] C Aslangul, N Pottier, and D Saint-James, “Quantum ohmic dissipation: cross-over between quantum tunnelling and thermally resisted motion in a biased tight-binding lattice,” *Journal de Physique* **47**, 1671–1685 (1986).
- [51] Aslangul, C., Pottier, N., and Saint-James, D., “Quantum brownian motion in a periodic potential: a pedestrian approach,” *J. Phys. France* **48**, 1093–1110 (1987).
- [52] Matthew P. A. Fisher and Wilhelm Zwerger, “Quantum brownian motion in a periodic potential,” *Phys. Rev. B* **32**, 6190–6206 (1985).

- [53] Julian Schwinger, “Brownian motion of a quantum oscillator,” *Journal of Mathematical Physics* **2**, 407–432 (1961).
- [54] Hermann Grabert, Peter Schramm, and Gert-Ludwig Ingold, “Quantum brownian motion: The functional integral approach,” *Physics Reports* **168**, 115 – 207 (1988).
- [55] Peter Hnggi and Gert-Ludwig Ingold, “Fundamental aspects of quantum brownian motion,” *Chaos: An Interdisciplinary Journal of Nonlinear Science* **15**, 026105 (2005).
- [56] Albert Schmid, “Diffusion and localization in a dissipative quantum system,” *Physical Review Letters* **51**, 1506 (1983).
- [57] Ulrich Weiss, Maura Sasseti, Thomas Negele, and Matthias Wollensak, “Dissipative quantum dynamics in a multiwell system,” *Zeitschrift für Physik B Condensed Matter* **84**, 471–482 (1991).
- [58] Marko Žnidarič, “Exact solution for a diffusive nonequilibrium steady state of an open quantum chain,” *Journal of Statistical Mechanics: Theory and Experiment* **2010**, L05002 (2010).
- [59] Viktor Eisler, “Crossover between ballistic and diffusive transport: the quantum exclusion process,” *Journal of Statistical Mechanics: Theory and Experiment* **2011**, P06007 (2011).
- [60] Marko Žnidarič and Martin Horvat, “Transport in a disordered tight-binding chain with dephasing,” *The European Physical Journal B* **86**, 67 (2013).
- [61] Xizhi Han and Sean A. Hartnoll, “Locality bound for dissipative quantum transport,” *Phys. Rev. Lett.* **121**, 170601 (2018).
- [62] Heinz-Peter Breuer and Francesco Petruccione, *The theory of open quantum systems* (Oxford University Press on Demand, 2002).
- [63] Edward Brian Davies, *Quantum theory of open systems* (Academic Press, 1976)

Quantum stochastic transport along chains

Dekel Shapira, Doron Cohen

(Supplementary Material)

===== [1] Ohmic dissipator for a two site system

Consider a two site system with Hamiltonian \mathbf{H}_0 and an Ohmic bath of temperature T that induces a fluctuating force $f(t)$ of intensity ν , and system-bath interaction term $-\mathbf{W}f(t)$. The master equation acquire a dissipation term

$$\mathcal{L}^{(\text{ohmic})}\rho = -\frac{\nu}{2}[\mathbf{W}, [\mathbf{W}, \rho]] - i\frac{\eta}{2}[\mathbf{W}, \{\mathbf{V}, \rho\}] \quad (\text{S-1})$$

where $\mathbf{V} = i[\mathbf{H}_0, \mathbf{W}]$, and $\eta = \nu/(2T)$. An extra noise source $\tilde{f}(t)V$ can be added in order to make the right hand side “positive” in the Lindblad sense:

$$\mathcal{L}^{(\tilde{\nu})}\rho = -\frac{\nu\eta}{2}[\mathbf{V}, [\mathbf{V}, \rho]] \quad (\text{S-2})$$

The “minimal correction” that is needed is to set $\nu_\eta = \nu/(4T)^2$, and then the expression can be written in the Lindblad form

$$\mathcal{L}^{(\text{ohmic})}\rho = \nu \left(\mathbf{F}\rho\mathbf{F}^\dagger - \frac{1}{2}\{\mathbf{F}^\dagger\mathbf{F}, \rho\} \right) - i[\mathbf{H}_{LS}, \rho] \quad (\text{S-3})$$

$$\mathbf{F} = \mathbf{W} + i\frac{\eta}{2\nu}\mathbf{V} \quad (\text{S-4})$$

$$\mathbf{H}_{LS} = \frac{\eta}{4}[\mathbf{W}\mathbf{V} + \mathbf{V}\mathbf{W}] \quad (\text{S-5})$$

where the Lamb-shift term \mathbf{H}_{LS} can be absorbed into the system Hamiltonian. For two site system with

$$\mathbf{H}_0 = -(\mathcal{E}/2)\sigma^z - (c/2)\sigma^x \quad (\text{S-6})$$

and coupling $\mathbf{W} = \sigma_x/2$, one has $\mathbf{V} = \mathcal{E}\sigma_y$, and the Lamb-shift is zero. The Lindblad generator is

$$\mathbf{F} = \left(1 + \frac{\mathcal{E}}{T}\right)\sigma^+ + \left(1 - \frac{\mathcal{E}}{T}\right)\sigma^- \quad (\text{S-7})$$

The transition rates between the sites are:

$$w^\pm = \left(1 \pm \frac{\eta\mathcal{E}}{2\nu}\right)^2 \nu \approx (\nu \pm \eta\mathcal{E}) \quad (\text{S-8})$$

$$\frac{w^-}{w^+} \approx e^{-\mathcal{E}/T} \quad (\text{S-9})$$

A secular-like (Pauli) version of the dissipator is obtained by expanding $\mathbf{F}\rho\mathbf{F}^\dagger$ and keeping only the Lindblad terms with $\mathbf{F}_+ = \sigma^+$ and $\mathbf{F}_- = \sigma^-$. Namely,

$$\mathcal{L}^{(\text{Pauli})}\rho = w^+ \left(\sigma^+\rho\sigma^- - \frac{1}{2}\{\sigma^-\sigma^+, \rho\} \right) + w^- \left(\sigma^-\rho\sigma^+ - \frac{1}{2}\{\sigma^+\sigma^-, \rho\} \right) - \frac{\gamma}{4}[\sigma^z, [\sigma^z, \rho]] \quad (\text{S-10})$$

where the last term represents excess noise due to noisy detuning (see below). The mixed terms that have been omitted affect only the decoherence of the off-diagonal terms, and not the rate of transitions between sites. In the Bloch-vector representation the precessing component of the “spin” decays only in the y direction in the Ohmic version, and isotropically in the Pauli version. In some sense the dissipation in the Pauli version assumes two independent baths at each bond. If we assume that the detuning \mathcal{E} is fluctuating with intensity $\nu_\gamma = (\gamma/2)$, so that $(\mathcal{E}/2) \rightarrow (\mathcal{E}/2) + f(t)$, then an additional \mathcal{L} term appears, that has the form of Eq.(S-1) with the substitution $\mathbf{W} := \sigma^z$, and $\mathbf{V} := -c\sigma^y$.

===== [2] Ohmic dissipator for a chain

The Hamiltonian of the chain is

$$\mathbf{H}^{(c)} = U(\mathbf{x}) - \frac{c}{2}(\mathbf{D} + \mathbf{D}^\dagger) = -\mathcal{E}\mathbf{x} - c \cos(\mathbf{p}) \quad (\text{S-11})$$

where $\mathbf{D} = \sum_x \mathbf{D}_x$ is the displacement operator, and $\mathbf{D}_x = |x+1\rangle\langle x|$. In general the field $\mathcal{E}_x = -(U(x+1) - U(x))$, as well as the hopping frequencies (c), and temperatures might be non-uniform. The interaction with a bath-source that induces non-coherent transitions at a given bond is obtained by the replacement $(c/2) \mapsto (c/2) + f(t)$. The baths of different bonds are uncorrelated. Accordingly the dissipation term in the Master equation takes the form

$$\mathcal{L}^{(\text{ohmic})}\rho = -\sum_x \left(\frac{\nu}{2} [\mathbf{W}_x, [\mathbf{W}_x, \rho]] + \frac{\eta}{2} i[\mathbf{W}_x, \{\mathbf{V}_x, \rho\}] \right) \quad (\text{S-12})$$

where the coupling to the baths is via the operators

$$\mathbf{W}_x = (\mathbf{D}_x + \mathbf{D}_x^\dagger) \quad (\text{S-13})$$

$$\mathbf{V}_x = i[\mathbf{H}^{(c)}, \mathbf{W}_x] = i\mathcal{E}_x (\mathbf{D}_x^\dagger - \mathbf{D}_x) - i\frac{c}{2} [(\mathbf{D}_{x+1}\mathbf{D}_x - \mathbf{D}_x\mathbf{D}_{x-1}) - h.c] \quad (\text{S-14})$$

And the Lindblad correction term:

$$\mathcal{L}^{(\bar{\nu})}\rho = -\frac{\nu\eta}{2} \sum_x [\mathbf{V}_x, [\mathbf{V}_x, \rho]] \quad (\text{S-15})$$

with intensity $\nu_\eta = \nu/(4T)^2$. Such term has negligible effect in the high temperature regime ($\eta < 1$). Optionally we can add terms that reflect fluctuations of the field. At a given bond it is obtained by the replacement $U(\mathbf{x}) \mapsto U(\mathbf{x}) + \tilde{f}(t)$, where $\tilde{f}(t)$ represents fluctuations of intensity γ . The implied coupling operators are

$$\mathbf{W}_x^{(S)} = \mathbf{Q}_x \quad (\text{S-16})$$

$$\mathbf{V}_x^{(S)} = i[\mathbf{H}^{(c)}, \mathbf{W}_x^{(D)}] = i(c/2) [\mathbf{D}_{x-1}^\dagger - \mathbf{D}_{x-1} - (\mathbf{D}_x^\dagger - \mathbf{D}_x)] \quad (\text{S-17})$$

===== [3] Expression for the current

For generality of the treatment we allow the temperature to be bond dependent, then $\eta \rightarrow \eta_x$ so that the Lindblad generators are $\mathbf{F}_x = \mathbf{W}_x + i(\eta_x/2\nu)\mathbf{V}_x$, and

$$\mathbf{H} = \mathbf{H}^{(c)} + \sum_x \frac{\eta_x}{4} \{\mathbf{W}_x, \mathbf{V}_x\} \quad (\text{S-18})$$

The time dependence of an expectation value is given by the adjoint equation:

$$\frac{d}{dt} \langle \mathbf{Q} \rangle = \text{trace} \left[\mathbf{Q} \frac{d}{dt} \rho \right] = \text{trace} [\mathbf{Q} \mathcal{L} \rho] = \text{trace} [(\mathcal{L}^\dagger \mathbf{Q}) \rho] = \langle \mathcal{L}^\dagger \mathbf{Q} \rangle \quad (\text{S-19})$$

where

$$\mathcal{L}^\dagger \mathbf{Q} = i[\mathbf{H}, \mathbf{Q}] + \nu \sum_x \left(\mathbf{F}_x^\dagger \mathbf{Q} \mathbf{F}_x - \frac{1}{2} \{ \mathbf{F}_x^\dagger \mathbf{F}_x, \mathbf{Q} \} \right) \quad (\text{S-20})$$

Partitioning the system at the n -th bond, the current flowing from left to right is defined by $I = \langle \dot{\mathbf{Q}} \rangle$, with

$$\mathbf{Q} = \sum_{x>n} |x\rangle\langle x| \quad (\text{S-21})$$

We note that although the original Hamiltonian allows only near-neighbor hopping, the master equation allows also “double hopping” due to the \mathbf{V} terms. Accordingly the expression for the current operator has several non-trivial

terms. Applying Eq.(S-19) the current is:

$$I = \vec{I} - \bar{I} - c \text{Im}[\rho_n(1)] + I_{\eta^2}^{(0)} + I_{\eta^2}^{(1)} \quad (\text{S-22})$$

$$\vec{I} = w_n^+ p_n - \frac{c\eta_n}{2} \text{Re}[\rho_{n-1}(1)] \quad (\text{S-23})$$

$$\bar{I} = w_n^- p_{n+1} - \frac{c\eta_n}{2} \text{Re}[\rho_{n+1}(1)] \quad (\text{S-24})$$

$$I_{\eta^2}^{(0)} = \frac{\mathcal{E}^2 \eta_n^2}{4\nu} [p_n - p_{n+1}] + \sum_{i=0,1} \frac{c^2}{16\nu} (\eta_{n-i}^2 + \eta_{n+1-i}^2) (p_{n-i} - p_{n+2-i}) \quad (\text{S-25})$$

$$I_{\eta^2}^{(1)} = -\frac{c\mathcal{E}}{8\nu} \text{Re} [2\eta_n^2 (\rho_{n-1}(1) + \rho_{n+1}(1)) - (\eta_{n-1}^2 + \eta_{n+1}^2) \rho_n(1)] \quad (\text{S-26})$$

where the extra I_{η^2} terms are of order η^2 , and are negligible for the NESS current. If the field \mathcal{E} is non-uniform, then one needs to make the replacement $\eta_n \mathcal{E} \rightarrow \eta_n \mathcal{E}_n$. Disregarding I_{η^2} the distinct elements of the current are coherent hopping, stochastic hopping and stochastic-assisted coherent hopping. These are pictured in Fig.S1.

Current in disordered system.– In Fig.S2 we display results for the NESS current, calculated for a disordered sample. If the spatial correlation scale of the disorder is large, the ring can be regarded as composed of several segments connected in series. Then the analytical estimate for the current would be

$$I = \left[\sum_x \frac{1}{v(\mathcal{E}_x)} \right]^{-1} \quad (\text{S-27})$$

which reduce to $I = (1/L)v(\mathcal{E})$ for a uniform field. The function $v(\mathcal{E})$ is provided by Eq.(17), and the above analytical estimate implies what we call *convex property*. Using this formula we can explain why disorder can lead to increase of the current as in Fig.2. The accuracy of this formula, that assumes a large spatial correlation scale, is tested against the correlation scale in Fig.S2.

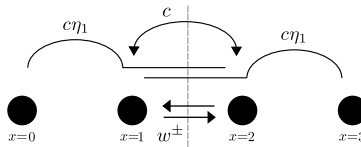


FIG. S1. Diagrammatic representation of the terms that contributes to the total current that flows via a section that is indicated by a vertical dashed line, here via the bond that connects sites $x=1$ and $x=2$. Straight lines denotes the role played by the stochastic transitions, while semi-circle segments are related to coherent hopping. The latter are of the form $c\eta_x \rho_x(1)$.

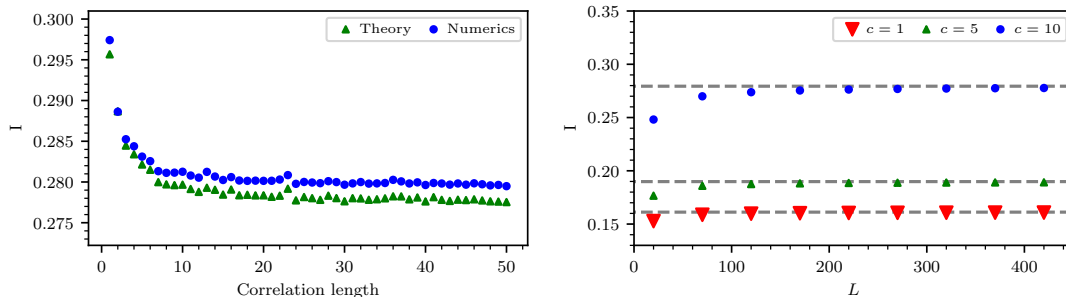


FIG. S2. The NESS current as a function of the correlation length of the disorder. The parameters are $\mathcal{E}=8$, $\sigma_{\mathcal{E}}=6$, $\eta=0.01$ and $c=10$. The correlated disorder is obtained by a convolution of the uncorrelated disorder (correlation length equals unity) with a box-shaped kernel. For each sample the numerical result for an $L=500$ ring is compared with the theoretical estimate Eq.(S-27). The two are expected to coincide for large correlation length. The small difference that remains is a finite size effect due to our treatment of the boundary conditions (see main text). On the right panel we demonstrate the L -dependence of this difference for a clean system (\mathcal{E} and η are the same). The gray dashed lines are the theoretical values provided by Eq.(17).

===== [4] Spreading

Without coherent hopping ($c=0$) the Ohmic/Pauli dynamics of the on-site probabilities p_x decouple from the decay of the off-diagonal terms. We get two distinct sets of modes: the stochastic-like relaxation modes and the off-diagonal decoherence modes. In the Pauli approximation the latter decay with the *same* rate $\gamma_0 = \gamma + w^+ + w^-$. The stochastic transitions affect only the stochastic-like relaxation modes. Starting with a wavepacket of variance $\text{Var}(R) = \sigma_0^2$, and momentum centered around k_0 , we get in the Wigner representation

$$\rho_w(R, P) = e^{-\gamma_0 t} [G^c(R, P) - G^0(R, P)] + G^t(R, P) \quad (\text{S-28})$$

where

$$G^c(R, P) = \frac{2}{L} \exp\left(-\frac{1}{2} \frac{R^2}{\sigma_0^2} - (P - k_0(t))^2 \sigma^2\right), \quad k_0(t) = k_0 + \mathcal{E}t \quad (\text{S-29})$$

$$G^t(R, P) = \frac{1}{\sqrt{2\pi}} \frac{1}{\sqrt{\sigma_0^2 + 2Dt}} \exp\left(-\frac{1}{2} \frac{(R - vt)^2}{\sigma_0^2 + 2Dt}\right) \quad (\text{S-30})$$

with drift velocity $v = (w^+ - w^-)$ and diffusion coefficient $D = (w^+ + w^-)/2$.

Let us add coherent hopping in a very naive way: we use the Pauli dissipator, and merely set $c \neq 0$ in the Hamiltonian. It is a naive procedure because the use of the Pauli dissipator cannot be justified anymore (we have to use the Ohmic dissipator). With this simplification the explicit form of the Lindblad operator of the q block is:

$$\mathcal{L}^{(q)} = -\gamma_0 + \gamma_q |0\rangle\langle 0| - i\mathcal{E} \sum_r |r\rangle r \langle r| - c \sin(q/2) \left[e^{iq/2} \mathcal{D}_\perp - e^{-iq/2} \mathcal{D}_\perp^\dagger \right] \quad (\text{S-31})$$

with $\gamma_q = \gamma + w^+ e^{-iq} + w^- e^{iq}$. This can be regarded as simplified version of Eq.(S-33) below. The diagonalization of \mathcal{L} is straightforward for zero bias. The phases $\exp(\pm iq/2)$ can be gauged to some distant r , and \mathcal{L} becomes like the Hamiltonian of a tight-binding model with a barrier at the origin. The lowest eigenmodes are decaying exponents $\psi(r) \sim \exp(-\alpha|r|)$, with $\text{Re}(\alpha) > 0$. These modes correspond to the stochastic-like relaxation modes. Matching the boundary conditions at $r = 0$, one finds the eigenvalues

$$\lambda_{q,0} = \gamma_0 - \sqrt{\gamma_q^2 - 4c^2 \sin^2(q/2)} \equiv ivq + Dq^2 + O(q^3) \quad (\text{S-32})$$

From which expressions for v and D can be derived. The result for D is similar (but not identical) to the correct result in the main text. Namely, up to a prefactor it reproduces the $\mathcal{E}=0$ Drude term.

===== [5] Bloch representation of the Ohmic master equation

For a clean system, and neglecting the η^2 contribution, the generator of the master equation is written as a sum of several terms. Here we shall provide explicit expressions of the q block of the super-matrix in the Bloch representation:

$$\mathcal{L}^{(q)} = c\mathcal{L}^{(c)} + \mathcal{E}\mathcal{L}^{(\mathcal{E})} + \nu\mathcal{L}^{(\nu)} + \eta c\mathcal{L}^{(\tilde{c})} + \eta\mathcal{E}\mathcal{L}^{(\tilde{\mathcal{E}})} + \nu\eta\mathcal{L}^{(\tilde{\nu})} \quad (\text{S-33})$$

We define operators

$$R = \sum_r |r\rangle r \langle r| \quad (\text{S-34})$$

$$\mathcal{D}_\perp = \sum_r |r+1\rangle \langle r| \quad (\text{S-35})$$

After gauge transformation $|r\rangle \rightarrow e^{-iqr/2} |r\rangle$ we obtain

$$\mathcal{L}^{(c)} = \sin(q/2) [\mathcal{D}_\perp^\dagger - \mathcal{D}_\perp] \quad (\text{S-36})$$

$$\mathcal{L}^{(\mathcal{E})} = -iR \quad (\text{S-37})$$

$$\mathcal{L}^{(\nu)} = -2 + 2 \cos(q) |0\rangle\langle 0| + (|1\rangle\langle -1| + |-1\rangle\langle 1|) \quad (\text{S-38})$$

$$\mathcal{L}^{(\tilde{c})} = \frac{1}{2} \cos(q/2) [\mathcal{D}_\perp + \mathcal{D}_\perp^\dagger] + \frac{1}{2} \cos(3q/2) [| \pm 1\rangle\langle 0| - |0\rangle\langle \pm 1|] + \frac{1}{2} \cos(q/2) [| \mp 2\rangle\langle \pm 1| - | \pm 1\rangle\langle \mp 2|] \quad (\text{S-39})$$

$$\mathcal{L}^{(\tilde{\mathcal{E}})} = -2i \sin(q) |0\rangle\langle 0| \quad (\text{S-40})$$

Note that this expression is not 2π periodic, since we ignore the accumulated phase which arise in the gauge procedure. The gauge in the above procedure is equivalent to redefinition of the r coordinate such that x and r become orthogonal (skewing the r axis in Fig.4 by 45 degrees).

[6] Eigenmodes of the Ohmic master equation

Infinite temperature eigen-modes.— For infinite temperature ($\eta = 0$), the eigenvalues of the $q = 0$ block are:

$$\lambda_{q=0,0} = 0 \text{ (NESS)} \quad (\text{S-41})$$

$$\lambda_{q=0,\pm} = 2\nu \pm \sqrt{\nu^2 - \mathcal{E}^2} \quad (\text{S-42})$$

$$\lambda_{q=0,s} = 2\nu + i\mathcal{E}s, \quad (s = \pm 2, \pm 3, \dots) \quad (\text{S-43})$$

Considering the q dependence of the eigenvalues we get several bands. Our interest below is in the lowest band ($\lambda_{q,s=0}$), which determines the long time spreading. For this calculation one needs the eigen-modes corresponding to the above eigenvalues. These are given by:

$$|\lambda_{q=0,s}\rangle = |r = s\rangle, \quad (s = 0, \pm 2, \pm 3, \dots) \quad (\text{S-44})$$

$$|\lambda_{q=0,\pm}\rangle \equiv |\pm\rangle = \alpha_{\pm} |1\rangle + |-1\rangle \quad (\text{unnormalized}) \quad (\text{S-45})$$

$$\alpha_{\pm} = -i \left(\frac{\mathcal{E}}{\nu} \right) \mp \sqrt{1 - \left(\frac{\mathcal{E}}{\nu} \right)^2} \quad (\text{S-46})$$

NESS at finite temperature.— We can find the NESS, which is the zero mode ($|\lambda_{0,0} = 0\rangle$), and calculate from it both the momentum distribution and the current.

Setting $q = 0$, and considering linear order in η , the NESS is obtained by first order perturbation for the $|\lambda_{q=0,0}\rangle = |r = 0\rangle$ state. See Fig.S3. Putting $V \equiv \eta c \mathcal{L}^{(c)}$ as the perturbation, one get:

$$|\text{NESS}\rangle = |0\rangle + \frac{\langle \tilde{+} | V | 0 \rangle}{\lambda_+} |+\rangle + \frac{\langle \tilde{-} | V | 0 \rangle}{\lambda_-} |-\rangle = |0\rangle + \alpha_0 |1\rangle + \alpha_0^* |-1\rangle \quad (\text{S-47})$$

$$\alpha_0 = \frac{3\nu - i\mathcal{E}}{3\nu^2 + \mathcal{E}^2} \eta c \quad (\text{S-48})$$

where the left eigenvectors are given by:

$$\langle \tilde{\pm} | = \left(\frac{\alpha_{\pm}}{\alpha_{\mp}} - 1 \right)^{-1} \left[\langle 1 | \frac{1}{\alpha_{\mp}} - \langle -1 | \right], \quad (\text{S-49})$$

Reverting back from the Bloch basis of $\rho(r; q)$ to the position basis, namely $|r; q\rangle := L^{-\frac{1}{2}} \sum_x |x\rangle \langle x+r| e^{iqx}$, the normalized steady state matrix ρ is:

$$\rho^{(\text{NESS})} = \frac{1}{L} \left(\mathbb{1} + \sum_x \alpha_0 |x\rangle \langle x+1| + h.c. \right) = \frac{1}{L} \left(\mathbb{1} + \alpha_0 e^{+ip} + \alpha_0^* e^{-ip} \right) \quad (\text{S-50})$$

The momentum distribution.— Using Eq.(S-50) we obtain the steady state momentum distribution:

$$p(k) = \rho_{kk} = \frac{1}{L} \left(1 + 2\text{Re}(\alpha_0 e^{+ik}) \right) = \frac{1}{L} + \frac{1}{L} \frac{2\eta c}{3\nu^2 + \mathcal{E}^2} (3\nu \cos(k) + \mathcal{E} \sin(k)) \quad (\text{S-51})$$

For $\mathcal{E} = 0$, the momentum distribution is canonical, see Fig.S4. The above result is indeed consistent with the canonical distribution to linear order in $\beta = 1/T$. The drift velocity can be deduced by calculating the NESS current using Eq.(S-22). The current over the bond n , to first order in η is:

$$I_n = \frac{1}{L} \left((w_n^+ - w_n^-) - c \text{Im}(\alpha_0) \right) = \frac{1}{L} \left[1 + \frac{c^2}{6\nu^2 + 2\mathcal{E}^2} \right] 2\eta \mathcal{E} \quad (\text{S-52})$$

We note that although the expression for the current Eq.(S-22) is complicated, the final NESS current is composed of the usual stochastic-current, and the usual coherent-current.

[7] Diffusion at finite temperature

Here we provide the calculation of D to second order in η . We have to expand $\lambda_{q,0}$ to second order in q . Inspecting the gauged Lindblad operator in Eq.(S-33), one observes (see diagram of Fig.S3) that up to order q^2 and η^2 it is enough to diagonalize the five sites $|r| \leq 2$, keeping the q^2 and the η^2 corrections. This can be done using perturbation theory, or optionally using *Mathematica* for a direct diagonalization and then expand the result in powers of q and η . Either way one get:

$$\lambda_{q,0} = ivq + Dq^2 \quad (\text{S-53})$$

$$v = \left[1 + \frac{c^2}{6\nu^2 + 2\mathcal{E}^2} \right] 2\eta\mathcal{E} \quad (\text{S-54})$$

$$D = \left[1 + \frac{c^2}{6\nu^2 + 2\mathcal{E}^2} \right] \nu - \left[\frac{(9\nu^2 + 11\mathcal{E}^2)}{(\mathcal{E}^2 + 3\nu^2)^2} + \frac{(15\mathcal{E}^2 + 13\nu^2)(c\mathcal{E})^2}{4(\mathcal{E}^2 + \nu^2)(\mathcal{E}^2 + 3\nu^2)^3} \right] (\eta c)^2 \nu \quad (\text{S-55})$$

Setting $\mathcal{E} = 0$ in the expression for D , we find that the η^2 correction in Eq.(S-55) can be absorbed into the first term via the replacement $c^2 \mapsto [1 - 6\eta^2]c^2$. Note that this correction is based on the Ohmic dissipator without the additional Lindblad term that is added for the purpose of positivity.

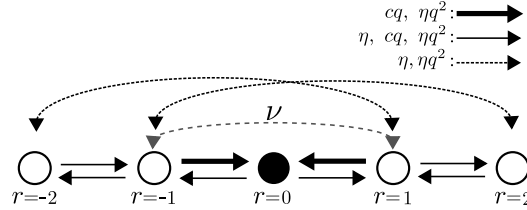


FIG. S3. Diagrammatic representation of the couplings in the reduced tight binding model (in r), that is used in order to determine the eigenvalues $\lambda_{q,s}$ for a given Bloch momentum q . Different orders of q and η are indicated by the different arrows. The formation of the $|\lambda_{q=0,\pm}\rangle$ eigenmodes is due to the dashed ν coupling. Up to order q^2 and η it is enough to consider second order perturbation theory involving $r = -1, 0, 1$. For η^2 corrections one needs to include also $r = \pm 2$.

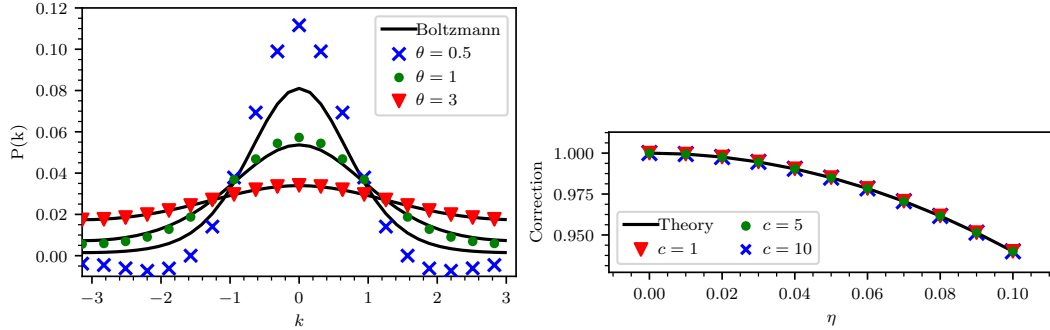


FIG. S4. The steady state and the diffusion coefficient at zero bias. The parameters are $\nu = 1$ and $\eta = 0.01$. (a) Numerically determined momentum distribution (without the Lindblad correction) compared with the Boltzmann distribution $p(k) \propto \exp[\theta^{-1} \cos(k)]$. The distribution is plotted for a few values of θ . For small θ the distribution is no longer Boltzmann-like and its tails become negative. The Ohmic master equation is no longer valid in this regime. The calculation is for $L = 40$, and for clarity only 20 data points are presented. (b) Numerical verification of the η^2 correction to D . The analytically predicted correction factor $[1 - 6\eta^2]$ is plotted as a solid line. The numerical data points are $[6\nu/c^2](D - \nu)$.

[8] Effective disorder

For $c=0$ the off-diagonal terms of ρ decouple from the diagonal, and the relaxation spectrum is the same as that of the stochastic model. For small c , we keep only the three-central diagonals ($r \leq 1$), thus ignoring the couplings to higher bands. We also ignore transitions of the order $c\eta$. The $r = \pm 1$ space can be eliminated, in the price of getting a λ -dependent transition rate matrix $H_{\text{eff}}(\lambda) = H_0 + W'G(\lambda)W$, where H_0 includes the transitions along $r=0$, and $G(\lambda)$ is a resolvent operator that describes the dynamics within the excluded diagonal, while the W -s include the couplings between the $r=0$ elements and the excluded $r = \pm 1$ elements. See diagram of the couplings in Fig.S5. The effective matrix $H_{\text{eff}}(\lambda)$ is non-hermitian due to the asymmetry of the transitions. It is a probability conserving tight-binding operator, but with rates that can be negative. For the forward and backward hopping rates in the n -th bond we get $w_n^\pm = \nu + \nu_n \pm \eta\mathcal{E}_n$, where

$$\nu_n = \left(\frac{c}{2}\right)^2 (G_{11} + G_{22} - G_{12} - G_{21}) = \frac{c^2}{2} \frac{\nu - \lambda}{(2\nu - \lambda)^2 + \mathcal{E}_n^2 - \nu^2} \quad (\text{S-56})$$

where $G = -(\lambda + L_n)^{-1}$ is a 2×2 matrix which is defined in terms of $L_n = -2\nu - i\mathcal{E}_n\sigma_z + \nu\sigma_x$ within the subspace that is spanned by the super-vectors $|n\rangle\langle n+1|$ and $|n+1\rangle\langle n|$. The eigenvectors of this matrix are the $|\pm\rangle$ of Eq.(S-46) with $\mathcal{E} \rightarrow \mathcal{E}_n$.

In order to estimate the effective disorder, we proceed as outlined in the main text. For high-temperatures one obtains from Eq.(22) approximations for the w_n and for the stochastic field, namely, $w_n \approx (\nu + \nu_n)$, and $\tilde{\mathcal{E}}_n \approx \eta\mathcal{E}(\nu + \nu_n)^{-1}$. We define an associated hermitian matrix \tilde{H} , that has the same matrix elements as $H_{\text{eff}}(\lambda)$, but with $\tilde{\mathcal{E}}_n = 0$ in the off diagonal elements. The eigenvalues of \tilde{H} are real, with some inverse localization length $\kappa(\lambda)$. Ignoring the diagonal disorder that arises due to non-uniform field $\tilde{\mathcal{E}}_n$, the localization length of eigenvalues near λ are roughly given by [Weinberg, de Leeuw, Kottos, Cohen, Phys. Rev. E 93, 062138 (2016)]:

$$\kappa(\lambda) \approx \frac{1}{4} \left(\frac{\sigma_\perp}{\nu}\right)^2 \frac{\lambda}{\nu} \quad (\text{S-57})$$

with $\sigma_\perp^2 = \text{Var}(w_n)$. This, as explained in the main text, determines whether the eigenvalues of $H_{\text{eff}}(\lambda)$ will turn complex. We focus on representative region around $\lambda = 2\nu$ in the center of the spectrum. Around this point, for small disorder, one obtains:

$$w_n \approx \nu \frac{c^2}{2(\nu^2 - \mathcal{E}^2)} (1 + B\delta_n + C\delta_n^2) \quad (\text{S-58})$$

$$B = \frac{2\mathcal{E}}{(\nu^2 - \mathcal{E}^2)}, \quad C = \frac{\nu^2 + 3\mathcal{E}^2}{(\nu^2 - \mathcal{E}^2)^2} \quad (\text{S-59})$$

with $\delta_n \equiv \mathcal{E}_n - \mathcal{E}$ that are randomly distributed within $[-\sigma_\mathcal{E}, \sigma_\mathcal{E}]$. Consequently we get the estimate

$$\sigma_\perp^2 = \text{Var}(w_n) \approx \left(\frac{c^2\nu}{2(\nu^2 - \mathcal{E}^2)}\right)^2 (B^2 \text{Var}(\delta) + C^2 \text{Var}(\delta^2)) = \left(\frac{c^2\nu}{2(\nu^2 - \mathcal{E}^2)}\right)^2 (B^2(\sigma^2/3) + C^2(4\sigma^4/45))$$

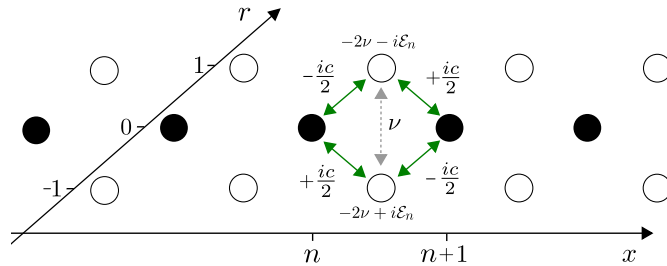


FIG. S5. Diagrammatic representation of the couplings in the 3 band approximation. Along the main diagonal (filled circles) we have asymmetric stochastic transitions (not indicated). Those are coupled to the coherences (empty circles) due to the c -related terms that are packed into W and W' matrices. The non-Pauli ν coupling and the on-site “energies” at the $|r| = 1$ sites constitute the L_n operator, which determines the resolvent $G(\lambda)$.